# Comparative Theoretical Study of CO Adsorption and Desorption Kinetics on (111) Surfaces of Transition Metals

**Ernst D. German* and Moshe Sheintuch**

*Department of Chemical Engineering, Technion—Israel Institute of Technology, Haifa 32000, Israel*

*Received: February 5, 2008; Revised Manuscript Received: June 22, 2008*

CO adsorption and desorption rates and adsorption equilibrium coefficients are analyzed for the processes on the close-packed metal surfaces of ruthenium, iridium, palladium, rhodium, and platinum assuming the adsorption to be activationless and using mobile and immobile adsorption layer models. Parameters required for calculations of the CO adsorption isotherm on these surfaces were studied using the ab initio density functional theory (DFT) cluster method with two correlation-exchange functionals. The adsorption energies, adsorption lengths, and metal−CO vibrational frequencies in the metal series were computed for two types of the adsorption sites, the on-top and the hollow hcp (hexagonal close-packed). Results of the calculations are compared with those obtained in other theoretical works and with experimental data. The application of the obtained results for catalysis is discussed.



## Introduction

Thermodynamic and kinetic adsorption characteristics of CO on various metals are important for several scientific and commercial applications: (i) Any kinetic model of a reaction involving CO either as a reactant (e.g., oxidation) or as a product (steam reforming) will require this information. (ii) Determining the surface diffusivity of CO requires its adsorption energy and other adsorption characteristics; in a future paper[1] we address this problem and use the results obtained here. (iii) CO is a strong inhibitor to hydrogen in fuel cells resulting in a requirement of a limiting concentration (less than 10 ppm CO in feed); predicting this limit and attempts to increase it by changing the anode metal will require absorption information. (iv) Specific surface area measurements of metal/support catalysts are based on selective CO adsorption on the metal; in this case it is important to find the stoichiometry of adsorption (i.e., M/CO ratio), since in dual-metal catalysts (e.g., Pd−Cu) it has been claimed that CO is adsorbed only on Pd and can be used for specific area measurements.[2]

Numerous theoretical and experimental works on various aspects of CO adsorption on close-packed transition metal surfaces have been published (see, for example, ref 3 and references therein). These works focused particularly on the M−CO bond lengths, the vibration frequencies and the adsorption energies, the electronic structure as well as the preferred adsorption site. Theoretical studies use density functional theory (DFT) methods in one of two main geometries that model the metal surface: the cluster and the slab. Periodic slab models have well-documented advantages when compared with the cluster approach,[4] which allow us, for example, to study adsorbate coverages effects and the collective properties of an adsorbate−adsorbent system in addition to the usual molecular quantum chemical characteristics. However, if one needs the adsorption energies, adsorption heights, and frequencies of M−CO vibrations only, simpler cluster models are proven to be appropriate, especially at the limit of zero coverage.[5] Good quality cluster models lead to almost the same values as those obtained with the periodic approaches but are computationally much less demanding (see, for example, the work of Gil et al.,[5] in which detailed numerical comparisons of both approaches were presented).

We note that studying the cross metal trend of CO adsorption characteristics should be interesting for catalysis and other technological applications. Trends in properties of CO adsorbed on a series of transition and noble metals were described using either periodic DFT methods with the gradient generalized approximation (GGA) of the exchange-correlation functionals[3−5] or using cluster models with the local density approximation (LDA).[6] The main purpose of the present work is to consider the trend in CO *kinetic* behavior, specifically, its rates of desorption and adsorption and the trend in the Langmuir adsorption isotherm coefficient on (111) metal surfaces. To that end we calculate the CO adsorption properties for the most stable adsorption states and derive the kinetics from it. In the next paper[1] we apply the results to the investigation of CO diffusivities on (111) metal surfaces.

Tabulation of published works (see below) shows that the adsorption characteristics depend on the employed experimental or theoretical method; this is especially true for the adsorption energy. Note that even a small variation in the adsorption energy on a certain metal due to different computation methods leads to a significant variation in estimated desorption rates, in desorption temperatures, and in the diffusion constants of adsorbed particles, since they depend exponentially on the adsorption energy. Thus, a comparative study of adsorption kinetics performed with the same method on various metals should reveal reliable trends even if the error associated with the individual data may be significant. Computation details are described in Appendix.

## Results and Discussion

In subsections 1−3 we consider shortly the characteristics of CO adsorption on surfaces of (111) metals, which are then used in subsection 4 for discussion of the adsorption kinetics.

**1. Adsorption Energies.** We list our findings of these characteristics in Tables 1 and 2.

* To whom correspondence should be addressed. E-mail: ernst_german@yahoo.com.

10.1021/jp801067h CCC: $40.75 
Published on Web 08/20/2008

**TABLE 1: CO On-Top Adsorption Energies (kcal/mol), Calculated from Cluster Models at the B3PW91/RPBE//LANL2DZ Level of the Theory[a] and Their Comparison with Published Data**

| Ru | Rh | Pd | Ir | Pt |
|---|---|---|---|---|
| | | This Study | | |
| −27.8/−31.4 | −34.3/−37.8 | −25.9/−30.7 | −34.4/−34.5 | −25.5/−30 |
| | | Published Experimental Data | | |
| −28.7 (ref 9)[b] | −34.6 (ref 12)[c] | | −44 ± 2 (ref 25)[e] | −31.7 (ref 29)[d] |
| −38.3 ± 1.5 (ref 9)[f] | −38.5 ± 1.4 (ref 13)[d] | | −38.3 (ref 26)[g] | −34.7 ± 4 (ref 30)[h] |
| | −32.8 (ref 14)[d] | | −35.9 (ref 27)[d] | −28 ± 1 (ref 31)[d,i] |
| | −31.6 (ref 15)[d] | | −35 ± 1 (ref 28)[j] | −27 (ref 32)[d] |
| | −31 (ref 16)[j] | | | −29.6 (ref 33)[k] |
| | −37 ± 1 (ref 17)[d] | | | −32 (ref 34)[l] |
| | | | | −34.9 (ref 34)[m] |
| | | | | −29.9 (ref 35)[n] |
| | | | | −32 ± 2 (ref 36)[d] |
| | | | | −27 ± 3.6 (ref 37)[o] |
| | | | | −31 ± 1 (ref 38)[n] |
| | | | | −38.3 ± 2 (ref 39)[p] |
| | | | | −33 (ref 40)[d] |
| | | | | −31 ± 1 (ref 41)[q] |
| | | | | −28.7 (ref 42)[r] |
| | | Published Theoretical Data for On-Top Site | | |
| −39/−42 (ref 3)[s,t] | −35.7/−42.9 (ref 3)[s,t] | −25.4/−32.5 (ref 7)[s,t,u] | −37.8/−44.7 (ref 3)[s,t] | −30.9/−38.5 (ref 3)[s,t] |
| −41.5 (ref 6)[s,v] | −39.4 (ref 6)[s,v] | −21 (ref 8)[w] | −48.9 (ref 6)[s,v] | −30.4 (ref 5)[x] |
| −41.5/−48 (ref 7)[s,t,u] | −40.6/−47.2 (ref 7)[s,t,u] | −23.5 to −28 (ref 21)[j,z] | −42.7/−48.7 (ref 7)[s,t,u] | −38.7 (ref 6)[s,v] |
| −27.2 (ref 8)[y] | −33.7 (ref 8)[w] | −30.4 (ref 22)[j] | −32.4 (ref 8)[y] | −31.1/−37.6 (ref 7)[s,t,u] |
| −41.2 (ref 10)[s,aa] | −36/−42.8 (ref 18)[s,ab] | −26.3/−33 (ref 23)[j,t] | | −26.5 (ref 8)[y] |
| −53 (ref 11)[w] | −38.7/−47 (ref 19)[j,t] | −30.0 (ref 24)[ac] | | −27 to −44 (ref 11)[w,z] |
| | −43.8 (ref 20)[ad] | | | −19 to −32.7 (ref 21)[j,z] |
| | | | | −33.4 (ref 24)[ac] |
| | | | | −33.7/−37.8 (ref 43)[j,ae] |
| | | | | −37.8 (ref 44)[o] |
| | | | | −36.7 (ref 45)[s] |
| | | | | −35.7 (ref 46)[s,af] |
| | | | | −43.1 (ref 47)[s,ag] |
| | | | | −26.3 (ref 75)[ah] |

[a] Metals arranged in periodic fashion; calculations on the 9/8/7 cluster. [b] Ru (001); $\theta > 1/3$. [c] $\theta = 0.18$. [d] Zero-coverage limit. [e] $\theta = 0.05$. [f] Ru (001); $0.05 < \theta < 0.33$. [g] $\theta = 0.04$. [h] $\theta = 0.17$. [i] Desorption kinetics; $E_{des}$ was extrapolated to zero coverage; initial experimental adsorption energy was found to be equal to −33 kcal/mol. [j] $\theta = 1/3$. [k] Calculated from desorption kinetics assuming prefactor equal to $10^{13}$ $s^{-1}$. [l] $\theta = 0.04$, atop adsorption is supposed to be more energy favorable. [m] $E_{des}$ was extrapolated to zero coverage with frequency factor equal to $1.25 \times 10^{15}$ $s^{-1}$. [n] $T = 350-1100$ K. [o] $\theta = 1/2$. [p] $0.17 < \theta < 0.33$. [q] $T = 350-415$ K. [r] $\theta = 0.05$. [s] $\theta = 1/4$. [t] RPBE/PW91. [u] We refer to "uncorrected" values of the authors in order to compare these results with other DFT calculations. [v] RPBE + AER. [w] 7/3 cluster. [x] Calculations on three-layer 52-atom cluster. [y] 7/6 cluster. [z] Depending on level of the theory. [aa] Ru(0001). [ab] GGA+U/standard GGA. [ac] Calculations at a fixed metal−CO distance of 1.94 Å and C−O bond of 1.14 Å. [ad] $\theta = 1/8$. [ae] B3LYP/PW91. [af] LDA geometry and PW91 energy. [ag] PW91. [ah] Calculations on (14/8/3) cluster.

***1.1. Palladium.*** CO hollow adsorption to the on-top position is preferable by 8 or 12 kcal/mol (calculated with the RPBE or B3PW91 functionals). The calculated hollow position adsorption energy (−38.3 kcal/mol) is quite close to the reported experimental value (−35.5 kcal/mol[48] at $\theta \rightarrow 0$), and it falls within the range of other published calculations of the hollow adsorption performed in the framework of both cluster and slab models (Table 2); this range is quite large and varies from about ∼ –27 to ∼ −47 kcal/mol, depending on the used functional. In the absence of any experimental information, our on-top adsorption energy is compared only with published theoretical data showing good agreement (Table 1).

***1.2. Iridium.*** The on-top adsorption having an energy of −34.4/−34.5 kcal/mol (B3PW91/RPBE) was found to be strongly preferable to the hollow one (Tables 1 and 2). This value should be compared to experimental finding of $E_{ads} = -35.9$ kcal/mol[27] (at $\theta \rightarrow 0$) or −35 ± 1 kcal/mol.[28] Our on-top adsorption energy is also within the range reported by other theoretical works, which vary between −32.4 and −48.9 kcal/mol (Table 1) with no clear dependence on coverage. In contrast to the on-top adsorption, the hollow adsorption energy depends strongly on type of the functional: −19.4 kcal/mol with B3PW91 and −24.5 kcal/mol with RPBE. Considerable effect of the functional on the iridium hollow adsorption energy was also obtained in ref 7.

***1.3. Rhodium.*** The calculated on-top adsorption energies, −37.8 kcal/mol (RPBE) or −34.3 kcal/mol (B3PW91), fall within the range of experimental data, shown in Table 1. The on-top adsorption is preferable to the hollow one (–31.4 (RPBE) to –32.7 (B3PW91) kcal/mol, Table 2) in accordance with experimental data[51] and in similarity to the trend obtained for iridium. Comparison of our result with other DFT theoretical studies shows that the site preference conclusion may vary with the approach employed. The RPBE exchange-correlation functional usually leads us to conclude that the on-top adsorption is more favorable,[6,8,19] whereas the PW91 exchange-correlation functional[3,7] results in the hollow adsorption being the most stable. Calculations[7] using the RPBE and PW91 functionals and involving a specific correction[52] to the adsorption energy support this conclusion.

***1.4. Platinum.*** CO adsorption on platinum was studied in many experimental and theoretical works. The adsorption

**TABLE 2: CO Hollow Adsorption Energies (kcal/mol), Calculated from Cluster Models at the B3PW91/RPBE//LANL2DZ Level of the Theory[a] and Their Comparison with Published Data**

| Ru | Rh | Pd | Ir | Pt |
|---|---|---|---|---|
| | | This Study | | |
| −25.2/−29.0 | −32.7/−31.4 | −38.3/−38.5 | −19.4/−24.5 | −26.3/−30.2 |
| | | Published Experimental Data | | |
| | −30 (ref 12)[b] | −35.5 (ref 48)[c] | | |
| | | −34 (ref 49)[b,d] | | |
| | | −36 (ref 86)[c] | | |
| | | Published Theoretical Data for Hollow Site | | |
| −39/−47 (ref 7)[e,f,g] | −36.2 (ref 6)[e,h] | −38.7/−48.2 (ref 3)[i,g] | −30/−37.8 (ref 7)[e,f,g] | −33.7 (ref 5)[j] |
| −42/−50 (ref 7)[k,f,g] | −37.6 (ref 6)[k,h] | −31.1 (ref 6)[e,h] | −33/−40.8 (ref 7)[k,f,g] | −34.4/−42.7 (ref 7)[l,f,g] |
| −21.7 (ref 8)[m] | −38/−46.4 (ref 7)[e,f,g] | −39/−48 (ref 7)[l,f,g] | −24.4 (ref 8)[m] | −27.7 (ref 8)[m] |
| −39.2 (ref 10)[k] | −40.4/−48.7 (ref 7)[k,f,g] | −26.5 (ref 8)[m] | | −23.5 to −27.4 (ref 21)[n,o] |
| | −31.4 (ref 8)[p] | −33 to −35 (ref 21)[n,o] | | −48.2 (ref 47)[i,q] |
| | −33.9/−44.6 (ref 18)[k,r] | −41.3 (ref 22)[n] | | |
| | −31.8/−42.1 (ref 18)[e,r] | −38/−46.4 (ref 23)[s,g] | | |
| | −35.5/−45.9 (ref 19)[k,g] | −37.6/45.4 (ref 23)[n,g] | | |
| | −33.4/−43.6 (ref 19)[e,g] | −36.9 (ref 50)[t,u] | | |
| | | −40.4 (ref 50)[t,v] | | |
| | | −36/−47.7 (ref 76)[e,g] | | |

[a] Metals arranged in periodic fashion; calculations on 6/7/6/5 cluster. [b] $\theta = 1/3$. [c] Zero-coverage limit. [d] Authors themselves assigned this value to bridge adsorption. [e] $\theta = 1/4$, fcc. [f] Here we refer to "uncorrected" values of the authors in order to compare these results with other direct DFT calculations. [g] RPBE/PW91. [h] RPBE + AER. [i] $\theta = 1/4$. [j] Calculations on 52-atom three-layer cluster; fcc. [k] $\theta = 1/4$, hcp. [l] $\theta = 1/4$, fcc and hcp. [m] 6/7 cluster. [n] $\theta = 1/3$, hcp. [o] Depending on level of the theory. [p] 6/7/3 cluster. [q] PW91. [r] GGA+U/standard GGA. [s] $\theta = 1/3$, fcc. [t] Calculations on 140-atomic cluster; BP86. [u] At relaxed Pd−Pd geometry. [v] At fixed Pd−Pd geometry.

energies were estimated from temperature-programed desorption (TPD) measurements[30−34,38,42] as well as from modulated molecular beam scattering,[35] laser-induced thermal desorption,[36] sum frequency generation vibrational spectroscopy (SFGVS),[37] single-crystal adsorption calorimetry,[39] and from high-resolution X-ray photoelectron spectroscopy (HR-XPS).[40] These estimations fall within a wide range of values (−27 to −38.3 kcal/mol). In the limit of low coverages, CO was found to adsorb mainly in the linear on-top coordinated sites,[31−36,38,40,42] and in this case the range of associated energy values is from −28 to −32 kcal/mol.

Our calculations with the RPBE functional lead to quite similar adsorption energies of the hexagonal close-packed (hcp) hollow and the on-top states (compare the corresponding data in Tables 1 and 2). The on-top adsorption energy (−30 kcal/mol) agrees very well with experimental data in the limit of low coverages. The binding energy of the hcp hollow state (−30.2 kcal/mol, RPBE) is slightly higher; we could not find relevant experimental information about this adsorption state, but the published theoretical results (Tables 1 and 2) suggest that the hcp hollow adsorption energy is slightly lower than the on-top adsorption energy, possibly by about 1.5 kcal/mol.

The variance between theoretical and experimental adsorption energies on platinum was discussed by several authors.[5,53,54] Gil et al.[5] applied various DFT computational methods using a series of cluster and periodic models and showed that both types of models, irrespective of the DFT approximation used, always favor CO adsorption at the threefold hollow site of platinum instead of CO adsorption at the on-top site.

***1.5. Ruthenium.*** We found the on-top adsorption site to be energetically more favorable than the hollow one by 2.5 kcal/mol (Tables 1 and 2). This preference is in agreement with other theoretical works.[3,6−8,10] The on-top adsorption energy calculated with the RPBE functional is still lower by ∼7 kcal/mol from the reported experimental value at $\theta = 1/3$.[9] The authors of that work attributed the obtained energy characteristic to the on-top adsorption, referring also to other publications where vibration spectrum[55] and low-energy electron diffraction (LEED) spectrum[56] of a similar system were studied. The CO on-top adsorption was claimed[9,55] to be preferable at coverage of $\theta = 1/3$. However, other studies[56] do not lead to clear conclusion about site preference at low coverage.

**2. Adsorption Lengths.** We present here calculations of the metal−CO adsorption lengths (or heights) (see the summary in Tables 3 and 4). The CO on-top adsorption lengths fall in a rather narrow domain (between 1.82 and 1.90 Å). This fact was previously pointed in other publications (see, for example, ref 3). Calculated heights are in agreement with experimental data and with most theoretical results referred in these tables. The hcp heights vary between metals more significantly than the on-top heights, from 1.25 for platinum to 1.57 Å for ruthenium. We can see that results of theoretical calculations of the on-top as well as the hcp heights on the same metal depend slightly on the used functional.

**3. Vibration Frequencies.** We found typical intervals of metal−carbon frequencies for the on-top and the hcp adsorbed states to fall between 430 and 500 $cm^{-1}$ and 340 and 370 $cm^{-1}$, respectively. This agrees in general with the corresponding data in ref 3. We failed to calculate accurately the Ru−CO normal vibrations frequency for the hcp position: the corresponding frequency includes an admixture of metal−metal vibrations and does not characterize exactly the metal−carbon normal vibration. It explains the rather low frequency value here, which was computed using the software of Gaussian 03. Correlation of the M−CO frequencies with the corresponding adsorption energies for the hollow (a) and the on-top (b) types (Figure 1) shows, as expected, that the $\omega$(M−CO) frequency declines with increasing (negative) adsorption energy, i.e., with increasing the metal−carbon bond strength.

**4. Specific Rate Constants of Desorption and Adsorption.** In this subsection the CO adsorption energies and frequencies (listed in Tables 1, 2, and 5) as well as the diffusion barriers calculated in ref 1 are applied for studying the CO specific rate constants of desorption and adsorption using the Eyring theory[72] (see also refs 73 and 74). According to this theory the specific rate constant of CO desorption may be calculated from the

**TABLE 3: Heights (angstroms) for On-Top Adsorbed CO Species, Calculated from Cluster Models at the B3PW91/RPBE// LANL2DZ Level of the Theory[a], and Their Comparison with Published Data**

| Ru | Rh | Pd | Ir | Pt |
|---|---|---|---|---|
| | | This Study | | |
| 1.898/1.893 | 1.845/1.838 | 1.831/1.822 | 1.880/1.890 | 1.846/1.838 |
| | | Published Experimental Data | | |
| 2. 0 ± 0.1 (ref 56)[b] | 1.87 ± 0.04 (ref 58)[b] | | | 1.85 (ref 60)[c] |
| 1.93 ± 0.04 (ref 57)[b] | 1.95 ± 0.1 (ref 59)[b] | | | |
| | | Published Theoretical Data for On-Top Site | | |
| 2.03 (ref 3)[d] | 1.99 (ref 3)[d] | 1.96 (ref 8)[e] | 1.85 (ref 6)[d] | 2.00 (ref 3)[d] |
| 1.90 (ref 6)[d] | 1.86 (ref 6)[d] | | 1.88 (ref 8)[e] | 1.84 (ref 6)[d] |
| 1.861 (ref 11)[f] | 1.86 (ref 8)[f] | | | 1.90 (ref 8)[e] |
| | 1.83 (ref 19)[b] | | | 1.862 to 1.904 (ref 11)[f,g] |
| | 1.845 (ref 20)[h] | | | 1.85 (ref 44)[i] |
| | | | | 1.85 (ref 46)[d] |
| | | | | 1.907 (ref 75)[j] |

[a] Metals arranged in periodic fashion. [b] $\theta = 1/3$. [c] $\theta \to 0$. [d] $\theta = 1/4$. [e] 7/6 cluster. [f] 7/3 cluster. [g] Depending on level of the theory. [h] $\theta = 1/8$. [i] $\theta = 1/2$. [j] 14/8/3 cluster.

**TABLE 4: Heights (angstroms) for hcp Adsorbed CO Species, Calculated from Cluster Models at the B3PW91/RPBE// LANL2DZ Level of the Theory[a] and Their Comparison with Published Data**

| Ru | Rh | Pd | Ir | Pt |
|---|---|---|---|---|
| | | This Study | | |
| 1.575/1.560 | 1.442/1.510 | 1.259/1.247 | 1.612/1.602 | 1.392/1.388 |
| | | Published Experimental Data Published Experimental Data | | |
| | | 1.29 ± 0.05 (ref 61)[b,c] | | |
| | | 1.27 ± 0.05 (ref 62)[b,c] | | |
| | | Published Theoretical Data for Hollow Sites | | |
| | 1.37/1.41 (ref 19)[d] | 1.31 (ref 3)[e] | | 1.33/1.37 (ref 43)[b,c,f] |
| | | | | 1.35/1.38 (ref 43)[b,f,g] |

[a] Metals arranged in periodic fashion; calculations on the 9/8/7 cluster. [b] $\theta = 1/3$. [c] fcc. [d] $\theta = 1/4$, fcc/hcp. [e] $\theta = 1/4$. [f] B3LYP/PW91. [g] hcp.

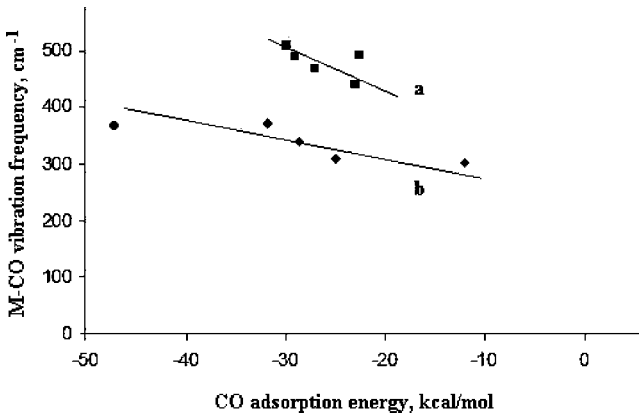


**Figure 1.** CO adsorption energy vs M−CO vibration frequency: (a) on-top adsorption, (b) hollow hcp adsorption.

equilibrium between adsorbed molecules and activated complexes, and it takes the form

$$k_{des} = \frac{k_B T}{h} \frac{F^*}{F_a} \exp[-E_{des}/k_B T] \quad (1)$$

where $F^*$ is the partition functions for the transition state, $F_a$ is the partition function for adsorbed molecules, and $E_{des}$ is the activation barrier for desorption. The explicit form of this equation depends strongly on the specific model assumed for desorption. Particularly, in a *mobile* adsorption layer model[72] (or a two-dimensional (2D) gaslike phase in Sellers[73] notation), which implies that the adsorbed molecule is not associated with a certain adsorption site, which seems to be appropriate when the desorption barriers are much larger than the diffusion barriers, the specific rate constant of desorption is given by eq 2[73]

$$k_{des} = \frac{k_B T}{h} \exp[(E_a^{dif} - E_{des})/k_B T] \quad (2)$$

where $E_a^{dif}$ is the barrier for CO surface diffusion and $F^*/F_a \sim 1$. The $E_a^{dif}/E_{des}$ ratio was studied in ref 1 and was found to be ~0.2 for CO adsorption on ruthenium, rhodium, iridium, and platinum and only 0.06 for palladium.

The adsorption rate (per second per square centimeter), assuming the process to be *activationless* and *indirect*, may be written as[72]

$$\tilde{k}_{ads} = \frac{k_B T}{h} \frac{p}{k_B T} \frac{F^*}{F_g} \quad (3)$$

where $F^*$ is the partition function per square centimeter of the activated complex, $F_g$ is the partition function for unit volume of gas, respectively, and $p$ is the gas phase pressure (in dyn/cm$^2$). The rate constant per one adsorption site is obtained by dividing $\tilde{k}_{ads}$ by the density of the adsorption centers/cm$^2$, which, for example, for an face-centered cubic (fcc) (111) surface is equal to $2.3094/d^2$,[73] where $d$ is the metal−metal distance (in cm). Since the activated complex is in the gas state, it will have vibrational and rotational degrees of freedom similar to the initial gas molecules. Therefore, the ratio of the partition functions $F^*/F_g$ reduces to the ratio of the translation terms. In the activated state a CO molecule has only two degrees of translation freedom, whereas in the gaseous state it has three such degrees of freedom. Thus, eq 3 takes the form

**TABLE 5: Stretching Metal−CO Vibration Frequencies ($cm^{-1}$), Calculated from Cluster Models at the B3PW91/RPBE// LANL2DZ Level of the Theory[a], and Their Comparison with Published Data**

| Ru | Rh | Pd | Ir | Pt |
|---|---|---|---|---|
| | | This Study: On-Top Adsorption[b] | | |
| 441\|429 | 509\|480 | 490\|501 | 467\|440 | 493\|507 |
| | | Published Data | | |
| 435 (ref 11)[c] | 468 (ref 17)[d] | | 505 (ref 3)[e] | 487 (ref 3)[e] |
| 445 (ref 54)[f] | 466/463 (ref 18)[e,g] | | | 390 to 449 (ref 11)[c,h] |
| 447 (ref 63)[i] | 507 (ref 20)[j] | | | 480 (ref 30)[k] |
| 436 (ref 64)[l] | 480 (ref 65)[d] | | | 475 (ref 38)[m] |
| | | | | 464 (ref 67)[n] |
| | | | | 460 (ref 68)[m] |
| | | | | 468 (ref 69)[s] |
| | | | | 476 (ref 70)[s] |
| | | | | 480 (ref 71)[s] |
| | | | | 409 (ref 75)[o,s] |
| | | This Study: hcp Adsorption[p] | | |
| (302)[q] | 340 | 370 | 311 | 372 |
| | | Published Data | | |
| | 390 (ref 17)[r] | 319 (ref 3)[e] | | 363 (ref 69)[g] |
| | 339 (ref 18)[e,g,s] | 322 (ref 66)[t] | | 350 (ref 71)[g] |

[a] Metals arranged in periodic fashion. [b] DFT calculations on 9/4/3|9/4/7 clusters. [c] DFT calculations on 7/3 cluster. [d] Exptl, $\theta \rightarrow 0$. [e] DFT calculations, $\theta = 0.25$. [f] Ru(001), exptl, $\theta = 0.2$. [g] Exptl, authors themselves attributed this frequency to the bridge adsorption; $\theta = 0.2$. [h] Depending on level of the theory. [i] Ru(001), exptl, $\theta = 0.33$. [j] DFT calculations, $\theta = 1/8$. [k] Exptl, $\theta = 0.17$. [l] Ru(0001), exptl, $\theta = 0.1$. [m] Exptl, low coverage. [n] Exptl, $\theta = 0.5$. [o] 14/8/3 cluster. [p] Calculations on 6/7/5 clusters. [q] This normal vibration includes an admixture of M−M vibrations. [r] Exptl, $\theta = 0.5$. [s] DFT calculation, $\theta = 1/4$, fcc. [t] Exptl, fcc.

**TABLE 6: Desorption Specific Rate Constants, $k_{des}$, Sticking Coefficients, $S_0$, and the Ratios $K = k_{ads}/k_{des}$ at $p = 10^5$ Pa[a]**

| item | Ru | Rh | Pd | Ir | Pt |
|---|---|---|---|---|---|
| $E_{des}$ (kcal/mol) | 31.4 | 37.8 | 30.7 | 34.5 | 30 |
| $E_a^{dif}$ (kcal/mol) | 6.0 | 6.3 | 2.2 | 6.9 | 6.4 |
| $k_{des}$ ($s^{-1}$) | 83 | 0.18 | $1.43 \times 10^{-3}$ | 9.07 | 508 |
| $k_{ads}$(indirect)/$k_{des}$ | $7.80 \times 10^5$ | $3.73 \times 10^8$ | $5.06 \times 10^{10}$ | $7.42 \times 10^6$ | $1.41 \times 10^5$ |
| $k_{ads}$(direct)/$k_{des}$ | $4.94 \times 10^3$ | $2.30 \times 10^6$ | $2.87 \times 10^8$ | $4.54 \times 10^4$ | $8.12 \times 10^2$ |
| $S_0$(direct) | 0.0064 | 0.0062 | 0.0057 | 0.0061 | 0.0058 |

[a] $T = 500$ K; $k_{ads}$ was calculated using eq 4 with $S_0 = 1$ (indirect adsorption) or with $S_0 < 1$ (direct adsorption) determined by eq 6; $k_{des}$ was calculated using eq 2.

$$k_{ads} = \frac{pd^2/2.3094}{\sqrt{2\pi m k_B T}} S_0 \quad (4)$$

where $m$ is the mass of the CO molecule (in g), and the sticking coefficient $S_0 = 1$.

In the case of *direct* adsorption the ratio $F^*/F_g$ in eq 3 reduces to

$$\frac{F^*}{F_g} = \frac{F^*(\text{vibr})}{F_g(\text{tr})F_g(\text{vibr})} = \frac{[(1-\exp[-h\nu/k_BT])^{-1}]^2}{(2\pi m k_B T)^{3/2}/h^3} \approx \frac{(k_BT/h\nu)^2 h^3}{(2\pi m k_B T)^{3/2}} \quad (5)$$

where the partition function $F_g$(vibr) is assumed to be equal to unity (for CO vibration); $\nu$ is the frequency of frustrated translation of CO adsorbed molecules parallel to the surface. This frequency is much lower than $k_BT/h$ justifying the approximation of the terms in square brackets of eq 5. Indeed, according to experimental measurements for CO adsorption on (111) platinum surface (see ref 1 and references therein) it lies in the range of 50−60 $cm^{-1}$. Our DFT calculation of normal vibrations for CO molecule adsorbed at the on-top site of rhodium (9/8/7) cluster yields the value of ~50 $cm^{-1}$, and other authors estimate (in harmonic approximation) the frequency to be in a range of 20−100 $cm^{-1}$ (see ref 1). Thus, the final expression for the rate constant (per second) for the direct adsorption can be written in the form of eq 4 with the dimensionless sticking coefficient $S_0$, which for an activationless process is equal to[74]

$$S_0 = \frac{2.3094}{d^2} \frac{(k_BT/h\nu)^2 h^2}{2\pi m k_B T} \quad (6)$$

With the use of eqs 2 and 4 and numerical values of the adsorption characteristics of Tables 1 and 2 along with the diffusion activation energies from ref 1, the specific rate constants of desorption ($k_{des}$) and the ratios $K = k_{ads}/k_{des}$ for low coverages were calculated for CO on the five metals at $T = 500$ K and at $p = 10^5$ Pa (Table 6 and Figure 2). Similarly to our calculations of diffusivities[1] the frequency of frustrated translations in these estimations was assumed to be the same for all metals (60 $cm^{-1}$). Accurate assignment of this frequency from normal coordinate analysis of CO/metal cluster complexes is a rather difficult problem because low-frequency vibrations in these systems consist of mixture of metal atoms and CO displacements.

We see from our calculations that the specific rate constant of desorption is the lowest and $K$ is the largest for the CO/palladium system. The desorption constants are high for Pt and Ru and extremely slow for Pd (desorption at 500 K will take an hour in order of magnitude). If Langmuir adsorption equilibrium is applied, the surface coverage $\theta$ under the

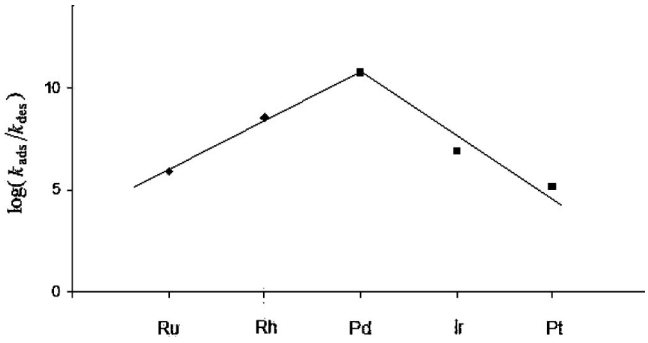


**Figure 2.** Variation of logarithms of the ratio $k_{ads}$(indirect)/$k_{des}$ ($p = 10^5$ Pa) for different metals at $T = 500$ K.

assumption of the indirect adsorption at 10 ppm (1 Pa) is $\theta = K/(1 + K) = 7.81/8.81 = 0.886$ for Ru and $1.56/2.56 = 0.609$ for Pt, whereas almost complete coverage is obtained at the other metals. In the direct adsorption model the sticking coefficient estimated by eq 6 is equal to 0.006 in the range of the considered metals leading to decrease of $K$ by ~160 times and to decrease the corresponding coverages. Note that in these calculations the CO adsorption energy on palladium is that which corresponds to the hollow adsorption as the more favorable (Table 2) and that on other metals corresponds to the on-top adsorption.

We end the paper by a remark concerning the use of our results in catalysis. The considered adsorption characteristics are important for various catalytic processes like hydrogen production in steam reforming and water gas shift and will be employed in further publications. They are also important to understand CO poisoning in fuel cells. Our results indicate the relative adsorption strength of the five metals. The uncertainty associated with calculation of adsorption constant (direct or indirect mode) is larger than the variation due to uncertainty in determining the adsorption energy. Since the correction due to the sticking coefficient ($S_0$) is constant, the relative strength is as indicated in Table 6. This table suggests that Rh and Pd are poisoned at 10 ppm CO at 500 K, using the direct or indirect adsorption mode.

## Conclusions

The relative CO adsorption strength on the five metals were investigated from first principles DFT method. The on-top adsorption is found to be the most favorable for ruthenium, rhodium, and iridium surfaces; the hollow position is preferable on palladium in agreement with published data. The energy difference between these sites at platinum (0.2 kcal/mol) is within the range of $k_BT$. The calculated adsorption energies of CO on the five metals, for the most stable site, fall within a range of ~ −30 to ~ −38 kcal/mol. It was shown that metal−CO vibration frequencies for the on-top and hollow adsorption decline with adsorption energies. This correlation allows using frequency data (which are simpler to measure than adsorption energies) for rough estimation of the adsorption energies. The calculated adsorption characteristics are used to describe CO desorption kinetics. The desorption constants are high for Pt and Ru and extremely slow for Pd due to its high adsorption strength and low activation barrier for the surface CO diffusion over this metal. The kinetic characteristics of CO adsorption on the considered metals vary sharply mainly due to changes in the adsorption energy. Data obtained suggests that Rh and Pd are poisoned at 10 ppm CO at 500 K, using the direct or indirect adsorption mode.

**Acknowledgment.** We thank Dr. E. Shustorovich for discussion of this work and his comments. This work was supported by the Israeli Science Foundation.

## Appendix: Computational Details

DFT calculations reported here were performed with the Gaussian 03 software package[77] on 24-atom clusters (Supporting Information, Figure S1): three-layer 9/8/7 clusters were applied for modeling the on-top adsorption, and four-layer 6/7/6/5 clusters were applied for modeling the hcp adsorption (Supporting Information, Figure S2). We used the Becke three-parameter hybrid functional (B3)[78] with the Perdew and Wang's 1991 gradient-corrected correlation functional (PW91)[79] and the RPBE functional of Hammer, Hansen, and Nørskov.[76] The RPBE functional was shown[3,76] to result in lower adsorption energies for CO as compared to the PW91 functional, the PBE[80] functional, and the revised PBE functional (revPBE),[81] improving systematically the agreement with experiment in most cases with almost unaffected geometrical structure. The exchange-correlation functional B3PW91 that was previously used in ref 82 leads to lower CO adsorption energies than the PW91 functional.

With the use of these functionals we calculated optimized values of metal−metal bond lengths in bare clusters, which are slightly lower than bulk experimental values as shown in Table S1 (Supporting Information).

The standard double-ζ basis set (LANL2DZ)[83] was used to describe the valence electrons of the metal atoms, whereas C and O atoms were described by the aug-cc-pVDZ basis set[84] including polarization and diffuse functions. This basis yields a CO bond length of 1.337 Å (vs the experimental value of 1.33 Å[85]) and a C−O frequency of 2194 $cm^{-1}$ (vs 2170 $cm^{-1}$ [85]).

It was shown[82] for $Cu_{18}CO$ cluster that, without adding diffuse functions to the basis set, the calculated adsorption energy suffers from a large basis set superposition error (BSSE) that would require a correction. The BSSE using a basis set which includes diffuse functions was negligible (only 0.05 eV). A small BSSE was also found[87] where the CO atop adsorption on copper clusters was investigated using the basis set with diffuse functions. Taking into account these results, in the present work we calculate the CO adsorption energies neglecting the effect of the BSSE.

Adsorption energies calculated by the cluster methodology are expected to be size-dependent and should converge for clusters of many layers. Thus, studying the energy size dependence is a necessary prerequisite for using the cluster models for adsorption calculations. Well-converged cluster calculations have been shown to yield results similar to those in periodic models. This convergence is most important when calculating adsorption energies and is less important for calculation of local properties such as the equilibrium bond distances and vibration frequencies, which depend on the gradient of potential energy.[5,8]

For on-top and hcp adsorption sites the energy and the geometry size dependencies were investigated using $Pd_n$ ($n = 13-24$) clusters and B3PW91 functional. The results of these calculations are shown in Figures S3−S6 (Supporting Information). One can see (Figures S3 and S4) that the adsorption energy converges to a value of ~38 kcal/mol for a cluster of 24 atoms or larger. The adsorption energy calculated on small clusters does not show smooth size dependence, and the corresponding results may, generally speaking, be unreliable. The size dependence of the adsorption height, on the other hand, does not show any sharp changes especially, and this is especially true for atop

adsorption. The curve characterizing the size dependence of the hollow adsorption slightly oscillates with very small amplitude. The CO bond length is essentially independent on the cluster size. It is, for example, equal to 1.147 Å when CO is on-top-adsorbed on three-layer clusters having from 14 to 24 metal atoms (note that the calculated bond length of a free CO molecule is equal to 1.134 Å as compared to experimental value 1.13 Å[85]).

The M−CO and C−O vibration frequencies are calculated in terms of harmonic analysis as it is implemented in Gaussian 03 software package. Since vibration frequencies depend rather weakly of cluster size[5,8,75] these calculations are performed (to save processor time) on 16- and 18-atom clusters for on-top and hcp sites.

**Supporting Information Available:** Geometrical structures of 24-atom model clusters, size dependencies, and a table of optimized metal−metal bond lengths. This material is available free of charge via the Internet at http://pubs.acs.org.

## References and Notes


(1) German, E. D.; Sheintuch, M.; Kuznetsov, A. M. *J. Phys. Chem. C* **2008**, *112*, in press.
(2) Efremenko, I.; Sheintuch, M. *Surf. Sci.* **1998**, *414*, 148.
(3) Gajdoš, M.; Eichler, A.; Hafner, J. *J. Phys: Condens. Matter* **2004**, *16*, 1141.
(4) van Santen, R. A.; Neurock, M. *Catal. Rev. Sci. Eng.* **1995**, *37*, 557.
(5) Gil, A.; Clotet, A.; Ricart, M. J.; Kresse, G.; Garcia-Hernandez, M.; Rösch, N.; Sautet, P. *Surf. Sci.* **2003**, *530*, 71.
(6) Liu, W.; Zhu, Y. F.; Lian, L. S.; Jiang, Q. *J. Phys. Chem. C* **2007**, *111*, 1005.
(7) Abild-Pedersen, F.; Andersson, M. P. *Surf. Sci.* **2007**, *601*, 1747.
(8) (a) Koper, M. T. M.; van Santen, R. A.; Wasileski, S. A.; Weaver, M. J. *J. Chem, Phys.* **2000**, *113*, 4392see also: (b) Wasileski, S.; Weaver, M.; Koper, M. T. M. *J. Electroanal. Chem.* **2001**, *500*, 344. (c) Koper, M. T. M.; van Santen, R. A. *J. Electroanal. Chem.* **1999**, *476*, 64.
(9) Pfnür, H; Feulner, P.; Menzel, D. *J. Chem. Phys.* **1983**, *79*, 4613.
(10) Stampfl, C.; Scheffler, M. *Phys. Rev. B* **2002**, *65*, 155417.
(11) Liao, M.-S.; Cabrera, C. R.; Ishikawa, Y. *Surf. Sci.* **2000**, *445*, 267.
(12) Smedh, M.; Beutler, A.; Borg, M.; Nyholm, R.; Andersen, J. N. *Surf. Sci.* **2001**, *491*, 115.
(13) Wei, D. H.; Skelton, D. C.; Kevan, S. D. *Surf. Sci.* **1997**, *381*, 49.
(14) Perterlinz, K. A.; Curtiss, T. J.; Sibener, S. J. *J. Chem. Phys.* **1991**, *95*, 6972.
(15) Thiel, P. A.; Williams, E. D.; Yates, J. T., Jr.; Weinberg, W. H. *Surf. Sci.* **1979**, *84*, 54.
(16) Castner, D. G.; Sexton, B. A.; Somorjai, G. A. *Surf. Sci.* **1978**, *71*, 519.
(17) (a) Linke, R.; Curulla, D.; Hopstaken, M. J. P.; Niemantsverdriet, J. W. *J. Chem. Phys.* **2001**, *115*, 8209. (b) Curulla, D.; Linke, R.; Clotet, A.; Ricart, J. M.; Niemantsverdriet, J. W. *Chem. Phys. Lett.* **2002**, *354*, 503.
(18) Köhler, L.; Kresse, G. *Phys. Rev. B* **2004**, *70*, 165405.
(19) Mavrikakis, M.; Rempel, J.; Greeley, J.; Hansen, L. B.; Nørskov, J. K. *J. Chem. Phys.* **2002**, *117*, 6737.
(20) Krenn, G.; Bako, I.; Schennach, R. *J. Chem. Phys.* **2006**, *124*, 144703.
(21) Philipsen, P. H. T.; van Lenthe, E.; Snijders, J. G.; Baerends, E. J. *Phys. Rev. B* **1997**, *56*, 13556.
(22) Seitsonen, A. P.; Kim, Y. P.; Schwegmann, S.; Over, H. *Surf. Sci.* **2000**, *468*, 176.
(23) Sacong, S.; Mosch, C.; Gross, A. *Phys. Chem. Chem. Phys.* **2007**, *9*, 2216.
(24) Hammer, B.; Morikawa, Y.; Nørskov, J. K. *Phys. Rev. Lett.* **1996**, *76*, 2141.
(25) Boyle, R. W.; Lauterbach, J.; Schick, M.; Mitchell, W. J.; Weinberg, W. H. *Ind. Eng. Chem. Res.* **1996**, *35*, 2986.
(26) Sushchikh, M.; Lauterbach, J.; Weinberg, W. H. *J. Vac. Sci. Technol., A* **1997**, *15*, 1630.
(27) Lauterbach, J.; Boyle, R. W.; Schick, M.; Mitchell, W. J.; Meng, B.; Weinberg, W. H. *Surf. Sci.* **1996**, *350*, 32.
(28) Comrie, C. M.; Weinberg, W. H. *J. Chem. Phys.* **1976**, *64*, 250.
(29) Poelsema, B.; Palmer, R. L.; Comsa, G. *Surf. Sci.* **1984**, *136*, 1.
(30) Steininger, H.; Lehwald, S.; Ibach, H. *Surf. Sci.* **1982**, *123*, 264.
(31) Ertl, G.; Neumann, M.; Streit, K. M. *Surf. Sci.* **1977**, *64*, 393.
(32) Collins, D. M.; Spicer, W. E. *Surf. Sci.* **1977**, *69*, 85.
(33) McCabe, R. W.; Schmidt, L. D. *Surf. Sci.* **1977**, *65*, 189.
(34) Campbell, C. T.; Ertl, G.; Kuipers, H.; Segner, J. *Surf. Sci.* **1981**, *107*, 207.
(35) Lin, T. H.; Somorjai, G. A. *Surf. Sci.* **1981**, *107*, 573.
(36) Seebauer, E. G.; Kong, A. C. F.; Schmidt, L. D. *J. Vac. Sci. Technol., A* **1987**, *5*, 464.
(37) Westerberg, S.; Wang, C.; Somorjai, G. A. *Surf. Sci.* **2005**, *582*, 137.
(38) Crowell, J. F.; Garfunkel, E. L.; Somorjai, G. A. *Surf. Sci.* **1982**, *121*, 303.
(39) Yeo, Y. Y.; Vattuone, L.; King, D. A. *J. Chem. Phys.* **1997**, *106*, 392.
(40) Kinne, M.; Fuhrmann, T.; Whelan, C. M.; Zhu, J. F.; Pantförder, J.; Probst, M.; Held, G.; Denecke, R.; Steinrück, H.-P. *J. Chem. Phys.* **2002**, *117*, 10852.
(41) Cudok, A.; Froitzheim, H.; Schulze, M. *Phys. Rev. B* **1993**, *47*, 13682.
(42) Norton, P. R.; Goodale, J. W.; Selkirk, E. B. *Surf. Sci.* **1979**, *83*, 189.
(43) Doll, K. *Surf. Sci.* **2004**, *573*, 464.
(44) Morikawa, Y.; Mortensen, J. J.; Hammer, B.; Norskov, J. K. *Surf. Sci.* **1997**, *386*, 67.
(45) Zhang, C. J.; Baxter, R. J.; Hu, P.; Alavi, A.; Lee, M.-H. *J. Chem. Phys.* **2001**, *115*, 5272.
(46) Bleakley, K.; Hu, P. *J. Am. Chem. Soc.* **1999**, *121*, 7644.
(47) Lynch, M.; Hu, P. *Surf. Sci.* **2000**, *458*, 1.
(48) Guo, X.; Yates, J. T., Jr *J. Chem. Phys.* **1989**, *90*, 6761.
(49) Conrad, H.; Ertl, G.; Koch, J.; Latta, E. E. *Surf. Sci.* **1974**, *43*, 462.
(50) Yudanov, I. V.; Sahnoun, R.; Neyman, K. M.; Rösch, N. *J. Chem. Phys.* **2002**, *117*, 9887.
(51) Beutler, A.; Lundgren, E.; Nyholm, R.; Andersen, J. N.; Setlik, B. J.; Heskett, D. *Surf. Sci.* **1997**, *371*, 381; **1998**, *396*, 117.
(52) Mason, S. E.; Grinberg, I.; Rappe, A. M. *Phys. Rev. B* **2004**, *69*, 161401.
(53) Feibelman, P. J.; Hammer, B.; Nørskov, J. K.; Wagner, F.; Scheffler, M.; Stumpfl, R.; Watwe, R.; Dumesic, J. *J. Phys. Chem. B* **2001**, *105*, 4018.
(54) Grinberg, I.; Yourdshahyan, Y.; Rappe, A. M. *J. Chem. Phys.* **2002**, *117*, 2264.
(55) Thomas, G. E.; Weinberg, W. H. *J. Chem. Phys.* **1979**, *70*, 954.
(56) Michalk, G.; Moritz, W.; Pfnür, H.; Menzel, D. *Surf. Sci.* **1983**, *129*, 92.
(57) Over, H.; Moritz, W.; Ertl, G. *Phys. Rev. Lett.* **1993**, *70*, 315.
(58) Gierer, M.; Barbieri, A.; Van Hove, M. A.; Somorjai, G. A. *Surf. Sci.* **1997**, *391*, 176.
(59) Koestner, R. J.; Van Hove, M. A.; Somorjai, G. A. *Surf. Sci.* **1981**, *107*, 439.
(60) Ogletree, D. F.; Van Hove, M. A.; Somorjai, G. A. *Surf. Sci.* **1986**, *173*, 351.
(61) Ohtani, H.; Van Hove, M. A.; Somorjai, G. A. *Surf. Sci.* **1987**, *187*, 372.
(62) Giessel, T.; Schaff, O.; Hirschmugl, C. J.; Fernandez, V.; Schindler, K.-M.; Theobald, A.; Bao, S.; Lindsay, R.; Berndt, W.; Bradshaw, A. M.; Baddeley, C.; Lee, A. F.; Lambert, R. M.; Woodruff, D. P. *Surf. Sci.* **1998**, *406*, 90.
(63) Jakob, P.; Persson, B. N. J. *Phys. Rev. Lett.* **1997**, *78*, 3503.
(64) He, P.; Dietrich, H.; Jacobi, K. *Surf. Sci.* **1996**, *345*, 241.
(65) Dubois, L. H.; Somorjai, G. A. *Surf. Sci.* **1980**, *91*, 514.
(66) Surnev, S.; Sock, M.; Ramsey, M. G.; Netzer, F. P.; Wiklund, M.; Borg, M.; Andersen, J. N. *Surf. Sci.* **2000**, *470*, 171.
(67) Surman, M.; Hagans, P. L.; Wilson, N. E.; Baily, C. J.; Russel, A. E. *Surf. Sci.* **2002**, *511*, L303.
(68) Gorte, R. J.; Schmidt, L. D. *Surf. Sci.* **1981**, *111*, 260.
(69) Froitzheim, H.; Hopster, H.; Ibach, H.; Lehwald, S. *Appl. Phys.* **1977**, *13*, 147.
(70) Hopster, H.; Ibach, H. *Surf. Sci.* **1978**, *77*, 109.
(71) Baro, A. M.; Ibach, H. *J. Chem. Phys.* **1979**, *71*, 4812.
(72) Glasstone, S.; Laidler, K. J.; Eyring, H. *The Theory of Rate Processes*; McGraw-Hill: New York, 1941.
(73) Sellers, H. *Russ. J. Phys. Chem. B* **2007**, *1*, 377.
(74) Chorkendorff, I.; Niemantsverdriet, J. W. *Concepts of Modern Catalysis and Kinetics*; Wiley-VCH Verlag GmbH&Co.: Weinheim, Germany, 2003.
(75) Curulla, D.; Clotet, A.; Ricart, J. M.; Illas, F. *J. Phys. Chem. B* **1999**, *103*, 5246.
(76) Hammer, B.; Hansen, L. B.; Nørskov, J. K. *Phys. Rev. B* **1999**, *59*, 7413.
(77) Frisch, M. J.; Trucks, G. W.; Schlegel, H. B.; Scuseria, G. E.; Robb, M. A.; Cheeseman, J. R.; Montgomery, J. A., Jr.; Vreven, T.; Kudin, K. N.; Burant, J. C.; Millam, J. M.; Iyengar, S. S.; Tomasi, J. J.; Barone, V.; Mennucci, B.; Cossi, M.; Scalmani, G.; Rega, N.; Petersson, G. A.; Nakatsuji, H.; Hada, M.; Ehara, M.; Toyota, K.; Fukuda, R.; Hasegawa, J.; Ishida, M.; Nakajima, T.; Honda, Y.; Kitao, O.; Nakai, H.; Klene, M.; Li,

X.; Knox, J. E.; Hratchian, H. P.; Cross, J. B.; Adamo, C.; Jaramillo, J.; Gomperts, R.; Stratmann, R. E.; Yazyev, O.; Austin, A. J.; Cammi, R.; Pomelli, C.; Ochterski, J. W.; Ayala, P. Y.; Morokuma, K.; Voth, A.; Salvador, P.; Dannenberg, J. J.; Zakrzewski, V. G.; Dapprich, S.; Daniels, A. D.; Strain, M. C.; Farkas, O.; Malick, D. K.; Rabuck, A. D.; Raghavachari, K.; Foresman, J. B.; Ortiz, J. V.; Cui, Q.; Baboul, A. G.; Clifford, S.; Cioslowski, J.; Stefanov, B. B.; Liu, G.; Liashenko, A.; Piskorz, P.; Komaromi, I.; Martin, R. L.; Fox, D. J.; Keith, T.; Al-Laham, M. A.; Peng, C. Y.; Nanayakkara, A.; Challacombe, M.; Gill, P. M. W.; Johnson, B.; Chen, W.; Wong, M. W.; Gonzalez, C.; Pople, J. A. *Gaussian 03*, revision B.05; Gaussian, Inc.: Pittsburgh, PA, 2003.

(78) Becke, A. D. *J. Chem. Phys.* **1993**, *98*, 5648.

(79) Perdew, J. P.; Chevary, J. A.; Vosko, S. H.; Jackson, K. A.; Pederson, M. R.; Singh, D. J.; Fiolhais, C. *Phys. Rev. B* **1992**, *46*, 6671.

(80) Perdew, J. P.; Burke, K.; Ernzerhof, N. *Phys. Rev. Lett.* **1996**, *77*, 3865.

(81) Zhang, Y.; Yang, W. *Phys. Rev. Lett.* **1998**, *80*, 890.

(82) Sudhyadhom, A.; Micha, D. A. *J. Chem. Phys.* **2006**, *124*, 101102.

(83) Hay, P. J.; Wadt, W. R. *J. Chem. Phys.* **1985**, *82*, 299.

(84) Woon, D. E.; Dunning, T. H., Jr *J. Chem. Phys.* **1993**, *98*, 1358.

(85) *Handbook of Chemistry and Physics*, 81st ed.; CRC Press: Boca Raton, FL, 2000−2001.

(86) Szymanski, P.; Harris, A. L.; Camillone, N., III. *J. Phys. Chem. A* **2007**, *111*, 12524.

(87) Wang, G.-C.; Jiang, L.; Morikawa, Y.; Nakamura, J.; Cai, Z.-Sh.; Pan, Y.-M.; Zhao, X.-Zh. *Surf. Sci.* **2004**, *570*, 205.

JP801067H